SEMICONDUCTOR STRUCTURES, LOW-DIMENSIONAL SYSTEMS, AND QUANTUM PHENOMENA

Silicon-on-Insulator Structures with a Nitrogenated Buried SiO$_2$ Layer: Preparation and Properties

I. E. Tyschenko^ and V. P. Popov

Rzhanov Institute of Semiconductor Physics, Siberian Branch, Russian Academy of Sciences, Novosibirsk, 630090 Russia
^e-mail: tys@isp.nsc.ru
Submitted August 2, 2010; accepted for publication August 25, 2010

Abstract—Electrical properties of silicon-on-insulator (SOI) structures with buried SiO$_2$ layer implanted with nitrogen ions are studied in relation to the dose and energy of N$^+$ ions. It is shown that implantation of nitrogen ions with doses $>3 \times 10^{15}$ cm^{-2} and an energy of 40 keV brings about a decrease in the fixed positive charge in the oxide and a decrease in the density of surface stares by a factor of 2. An enhancement of the effect can be attained by lowering the energy of nitrogen ions. The obtained results are accounted for by interaction of nitrogen atoms with excess silicon atoms near the Si/SiO$_2$ interface; by removal of Si—Si bonds, which are traps of positive charges; and by saturation of dangling bonds at the bonding interface of the SOI structure.

DOI: 10.1134/S1063782611030201

1. INTRODUCTION

The main limitation of the range of practical applications of silicon-on-insulator (SOI) structures consists in accumulation of charge in the insulator. Free holes generated in the valence band of SiO$_2$ are captured at the Si/SiO$_2$ interface. Positive charges thus localized at or near the interface represent, as a rule, "slow states," which feature large time constants and can be slowly charged or discharged when positive or negative bias is applied. Accumulation of such "anomalous positive charges" often brings about degradation of insulating SiO$_2$ [1] and affects the parameters of devices in the upper layer of an SOI structure by limiting their temporal stability and reducing their radiation resistance.

Nitrogenation of the thermal oxide as a result of interaction of nitrogen with excess silicon brings about removal of silicon–silicon bonds [2]. This effect is used to reduce the concentration of hole traps in the insulator. Indeed, the data in numerous available publications indicate that nitrogenation of SiO$_2$ layers is an effective method for improving their electrical parameters [3–11]. As a result, larger values of breakdown voltages [3, 4] and a lowered density of states at the interface with silicon [5] are attained, current–voltage ($I–V$) and capacitance–voltage ($C–V$) characteristics are improved [6, 7], a barrier for boron diffusion from polycrystalline gate to subgate insulator is formed [8], and resistance to ionized radiation is increased [9–11]. Metal–insulator–semiconductor (MIS) structures with a double insulator have obtained recognition in production of *n*-channel radiation-resistant integrated circuits. In particular, the use of

intermediate silicon nitride layers was suggested as a method for eliminating the leakage currents that originate after irradiation of MIS devices based on silicon-on-sapphire structures [11]. Later, ion-synthesized SOI structures with a buried insulator composed of silicon oxide and nitride were formed [12]. Subsequent studies of radiation-resistant SOI structures were mainly related to improvement of the method of ion-beam synthesis with the aim of fabrication of SOI structures with a multilayered buried insulator composed of SiO$_2$ and Si$_3$N$_4$ layers [6, 12–15] with a buried layer of silicon oxynitride [16], as well as with a layer of buried SiO$_2$ modified by nitrogen ions [17]. The existing methods of formation of SOI structures with a nitrogenated buried SiO$_2$ layer feature a number of disadvantages that are inherent both in the method of ion synthesis and the method of ion implantation as a whole and are related to the fact that nitrogenation of buried SiO$_2$ by implantation of nitrogen ions through a detached silicon layer brings about generation of radiation defects in the silicon layer above the insulator and destruction of the Si/SiO$_2$ interface. This, in turn, is accompanied by accumulation of additional traps both in the silicon layer and at the interface. Therefore, a search for new solutions of the problem of nitrogenation of the buried SiO$_2$ layer in SOI structures remains quite urgent.

The aim of this study consisted in the investigation of the electrical properties of SOI structures formed by the method of hydrogen-assisted transfer of silicon films onto thermally grown SiO$_2$ films implanted with N$^+$ ions in relation to the dose and energy of nitrogen ions.

2. THEORY

Models of analysis of properties of the interface in the semiconductor−insulator−semiconductor (SIS) structures were considered in detail in previous publications [18, 19]. If a voltage V_G is applied to the film and the substrate of the n-Si/SiO$_2$/n-Si structure is grounded, the main equations describing the capacitive properties of such a structure can be written as [18]

$$V_G = \psi_{s2} - \psi_{s1} + V_{ox} + W_{12}, \qquad (1)$$

$$Q_T = Q_{s1} + Q_{it2} + Q_{f1} = -Q_{s2} - Q_{it2} - Q_{f2}, \qquad (2)$$

$$V_{ox} = Q_T/C_{ox}, \qquad (3)$$

where ψ_{s1} is the surface potential of the boundary of bonding of the SOI structure (between the silicon film and the buried SiO$_2$ layer), ψ_{s2} is the surface potential of the thermal Si/SiO$_2$ interface (between the buried SiO$_2$ layer and silicon substrate), Q_T is the total charge in the buried oxide, V_{ox} is the potential dropping across the buried oxide, W_{12} is the bulk potential difference between the film and the substrate, Q_{s1} and Q_{s2} are surface charges corresponding to the silicon layer and the silicon substrate, Q_{it1} and Q_{it2} are charges at the upper and lower boundaries of the Si/SiO$_2$ SOI structure, and Q_{f1} and Q_{f2} are the fixed charges in the oxide near the upper and lower boundaries of Si/SiO$_2$. The total capacitance C_T of an SIS structure can be written as

$$\frac{1}{C_T} = \frac{1}{C_{s1} + C_{it1}} + \frac{1}{C_{ox}} + \frac{1}{C_{s2} + C_{it2}}, \qquad (4)$$

where $C_{s1,2} = -dQ_{s1,2}/d\psi_{s1,2}$ is the corresponding surface capacitance (the subscript 1 refers to the silicon film, and subscript 2 refers to the Si substrate), $C_{it1,2} = -dQ_{it1,2}/d\psi_{s1,2}$ is the static capacitance of traps at the corresponding interface, and C_{ox} is the capacitance of the buried oxide.

As the voltage at the gate is varied, the surface potential at both interfaces changes. In this case, superposition of surface potentials is possible; this superposition is bound to depend not only on silicon properties, but also on the properties of interfaces. Introduction of a parameter taking into account the overlap of surface potentials makes it possible to reduce the equivalent circuit of an SIS structure to the equivalent circuit of a conventional MIS capacitor. This makes it possible to use all the main equations in the theory of an MIS capacitor for description of capacitive properties of each of interfaces in a SOI structure. In the case of negative biases applied to the gate (the silicon layer at the insulator is in the state of accumulation, while the substrate is in the state of depletion), the coefficient of overlap of the surface potentials is given by [18]

$$K_2(\psi_{s1}) \equiv \frac{d\psi_{s1}}{d\psi_{s2}}. \qquad (5)$$

By differentiating expression (2), the coefficient of overlap of the surface potentials can be reduced to the following form:

$$K_2(\psi_{s2}) = -\frac{C_{s2} + C_{it2}}{C_{s1} + C_{it1}}. \qquad (6)$$

In accordance with the theory of MIS structures [20], the dependence of the surface potential on the voltage applied to the gate can be expressed in terms of the surface capacitance, capacitance of the insulator, and capacitance of the traps of charges in the following way:

$$\frac{d\psi_{s2}}{dV_G} = -\frac{C_{ox}}{C_{s2} + C_{it2} + C_{ox}(1 - K_2)}. \qquad (7)$$

We now substitute expression (6) into (4) and use expression (7) to obtain

$$\frac{1}{C_T} = \frac{1}{C_{ox}} + \frac{1 - K_2}{C_{s2} + C_{it2}}. \qquad (8)$$

It is clearly seen from expression (8) that, at $K_2 = 0$, the expression for the total capacitance of a SIS structures transforms into the expression for the capacitance of a MIS capacitor. The corresponding expressions can be also obtained in the case of positive biases when the substrate is found in the state of enhancement and the silicon layer is found in the state of depletion.

3. EXPERIMENTAL

In Fig. 1, we show the schematic representation of formation of SOI structures with a buried SiO$_2$ layer nitrogenated by implantation of nitrogen ions. As an initial material, we used silicon wafers with n-type conductivity, resistivity of 5−10 Ω cm, and orientation (100). At first, a SiO$_2$ film with a thickness of 300 nm was thermally grown on the first wafer. Then, N$^+$ ions were implanted into the layer of silicon dioxide (Fig. 1a). In the first series of experiments, the ion energy was 40 keV and the ion dose was varied in the range (1−6) × 10^{15} cm^{-2}. In the second series of experiments, the dose of ions was fixed and was equal to 3 × 10^{15} cm^{-2}, while the ion energy was varied from 20 to 40 keV. The used energies of N$^+$ ions ensured the formation of Gaussian-like profiles with the maximum of the distribution at a depth from 70 to 130 nm, respectively; the content of nitrogen atoms at the maximum of distribution was 0.15−1.15 at %. Hydrogen ions with an energy of 140 keV and the dose of 2 × 10^{16} cm^{-2} were implanted into the second wafer (Fig. 1b). Then, in a vacuum chamber, the implanted sides of the wafers were joined with simultaneous exfoliation of the silicon layer over the internal hydrophobic surface formed by implantation of H$^+$ ions; this layer was then transferred from the second wafer to the first one (Fig. 1c). The processes of joining the wafers, exfoliation, and transfer of the silicon layer were accom-
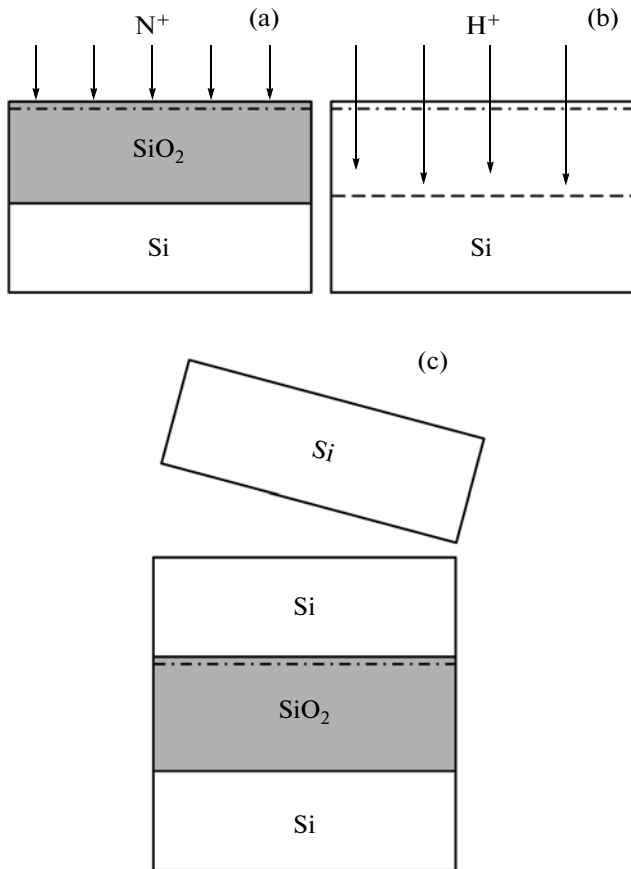
Fig. 1. Schematic representation of formation of an SOI structure with nitrogenated insulator: (a) implantation of N^+ ions into the SiO_2 layer grown thermally on the first wafer, (b) implantation of H^+ ions into the second wafer, and (c) bonding of implanted sides of the wafers and transfer of the Si layer.

Fig. 2. High-frequency (10^6 Hz) $C-V$ characteristics of the Al/n-Si/SiO$_2$/n-Si/Al structures with a SiO$_2$ layer (*1*) without introduced nitrogen and (*2–5*) after implantation of 40-keV N^+ ions with the doses (*2*) 1×10^{15}, (*3*) 2×10^{15}, (*4*) 3×10^{15}, and (*5*) 6×10^{15} cm^{-2}.

plished within a single stage at a temperature of 200°C in a vacuum chamber with a pressure of 10^2 Pa. The final annealing was performed for 1 h at a temperature of 1100°C. The thickness of the transferred Si layer was ~600 nm. Then, as a result of subsequent oxidation, the thickness of transferred silicon layer was made as large as 350–370 nm.

In order to assess the effect of nitrogen in the buried SiO$_2$ layer on electrical properties of SOI structures, we used the lithographic method to form the Al/n-Si/SiO$_2$/n-Si/Al mesa structures with the area of 700×700 μm. The thickness of the aluminum gate was 1000 nm. The capacitance–voltage ($C-V$) characteristics and dependences of the high-frequency conductivity on voltage (the $G-V$ characteristics) were measured at room temperature and at the frequency of the probing signal in the range 10^2–10^6 Hz. The bias was applied to the upper aluminum electrode; the back electrode (on the side of the substrate) was grounded.
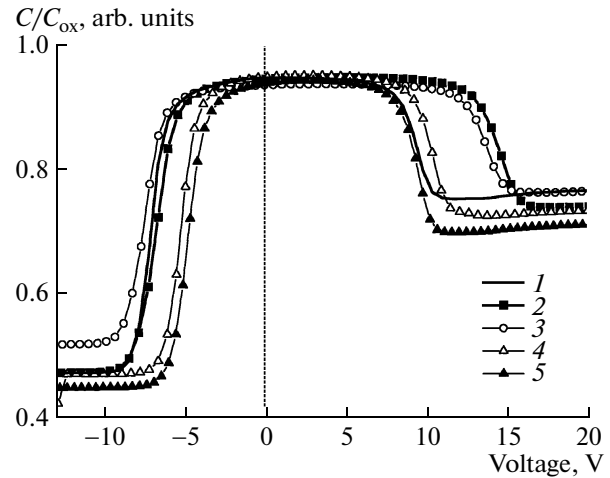
4. RESULTS AND DISCUSSION

In Fig. 2, we show the high-frequency (1 MHz) $C-V$ characteristics of the SOI capacitors, which do not contain nitrogen in the buried insulator, and also of the structures with the SiO$_2$ layer implanted with N^+ ions with the energy of 40 keV and doses of $1-6 \times 10^{15}$ cm^{-2} after annealing for 1 h at 1100°C. The characteristics shown in Fig. 1 are typical of semiconductor–insulator–semiconductor structures, which are represented by two MIS capacitors connected "back-to-back" [18]. In this case, the region of negative biases corresponds to the depletion mode and to inversion in the substrate, on the one hand, and to the accumulation mode for a top silicon layer, on the other hand. In contrast, the region of voltages at the gate >8 V corresponds to accumulation of the substrate with majority charge carriers and to depletion (with subsequent inversion) of the silicon layer. An analysis of the concentration of doping impurity on the basis of the minimum in the high-frequency capacitance yields a good agreement with the specified level of doping of the wafers used in the experiment.

It can be seen from Fig. 2 that implantation of nitrogen into the SiO$_2$ layer with doses $1-2 \times 10^{15}$ cm^{-2} brings about additional shifts of the flat-band voltage (V_{FB}) for the upper (V_{FB1}) and lower (V_{FB2}) MIS capacitors, which is indicative of an increase in the positive built-in charge in the insulator. A further increase in the nitrogen content in SiO$_2$ corresponding to an ion dose 3×10^{15} cm^{-2} and higher leads again to a negative shift of V_{FB} at positive values of the voltage applied to the gate; at the dose of N^+ ions 6×10^{15} cm^{-2}, the V_{FB} attains the value corresponding to the flat-band voltage for the structures that were not nitrogenated. In the region of negative voltages at the gate,

Table 1. The values of the flat-band voltage (V_{FB1} and V_{FB2}), the density of fixed charge (Q_{f1} and Q_{f2}), and the cross section σ_{n1} for the capture of majority charge carriers by the states at the interfaces of the SOI structures, which include the buried SiO_2 layer; the structures were implanted with 40-keV N^+ ions with the doses $1-6 \times 10^{15}$ cm^{-2} and were then annealed for 1 h at $1000°C$

Dose of N^+ ions, 10^{15} cm^{-2}	V_{FB1}, V	V_{FB2}, V	Q_{f1}, 10^{11}cm^{-2}	Q_{f2}, 10^{11}cm^{-2}	σ_{n1}, cm^2
0	8.1	−5.3	6.1	3.9	7.0×10^{-13}
1	13.0	−6.0	9.8	4.3	1.7×10^{-14}
2	12.2	−6.6	8.9	4.8	5.6×10^{-15}
3	9.1	−4.6	6.8	3.3	9.0×10^{-15}
6	8.3	−4.2	6.2	3.1	9.5×10^{-15}

V_{FB2} shifts in this case to positive values larger than those of the structures that were not nitrogenated; this is a consequence of a decrease in the density of positive charges in the insulator near the interface with the silicon substrate. It is worth noting that the density of fixed charge in the insulator of an SOI structure is determined independently in each part of the experimental $C-V$ curve, since application of a voltage corresponding to accumulation near one of interfaces yields a fixed charge in the oxide near the other interface. In our case, we determined the shift of the flat-band voltage from the difference between the experimental and theoretical values of V_{FB} obtained from intersection of linear portions of reverse square-law dependence of the total high-frequency capacitance in the depletion region for each of the interfaces with the
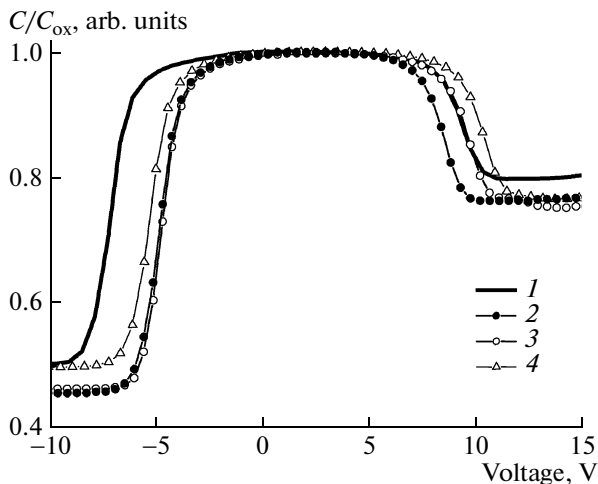

Fig. 3. The high-frequency (10^6 Hz) $C-V$ characteristics of the Al/n-Si/SiO$_2$/n-Si/Al structures with a SiO$_2$ layer (*1*) without introduced nitrogen and (*2–4*) after implantation of N$^+$ ions with the dose of 3×10^{15} cm^{-2} and energies of (*2*) 20, (*3*) 30, and (*4*) 40 keV.

line corresponding to capacitance of the insulator. Table 1 lists the values of V_{FB1}, V_{FB2}, and the density of the fixed charge in the insulator; these values are related to both of the interfaces (Q_{f1} and Q_{f2}).

In Fig. 3, we show the high-frequency (1 MHz) $C-V$ characteristics of the SOI capacitors, which do not contain nitrogen in the insulator layer, and also of the MIS structures with the SiO$_2$ layer implanted with N$^+$ ions at a dose of 3×10^{15} cm^{-2} (the ion energies were 20, 30, and 40 keV) and then annealed for 1 h at a temperature of $1100°C$. It can be seen that a decrease in the energy of nitrogen ions is accompanied by a positive shift of the flat-band voltage V_{FB2} in the region of negative biases and by a negative shift of V_{FB1} in the region of positive biases. The flat-band voltages and the densities of fixed charge in the oxide for each of considered cases are listed in Table 2.

The obtained results can be accounted for on the basis of experimental data obtained by the method of photoelectron spectroscopy [2]. According to these studies, excess overstoichiometric silicon exists in silicon oxide near the Si/SiO$_2$ interface. Excitation of excess Si–Si bonds can bring about the capture of holes and a fixed positive charge in the oxide. Nitrogenation of thermal oxide as a result of interaction of N atoms with excess silicon atoms leads to elimination of the Si–Si bonds. This effect is accompanied by a decrease in the concentration of hole traps in SiO$_2$. In the case under consideration, implantation of low doses of nitrogen is not sufficient for compensation of existing Si–Si bonds and leads only to generation of additional defects, including near the interface. Apparently, it is this effect that is the cause of an increase in the positive fixed charge in the structures implanted with low doses of N$^+$ ions. An increase in the ion dose to $4-6 \times 10^{15}$ cm^{-2} is found to be sufficient for compensation of Si–Si bonds near the interfaces by formation of Si–N–Si and Si–N–O bonds, as a result of which we observe a decrease in the positive fixed charge in the insulator near the Si/SiO$_2$ interfaces.

In Fig. 4, we show the $C-V$ and $G-V$ characteristics of the structures that did not contain nitrogen in the buried SiO$_2$ layer; the characteristics were measured at frequencies of $5 \times 10^2 - 5 \times 10^5$ Hz. It can be seen that, in the region of negative voltages at the gate >4 V corresponding to the depletion mode and the onset of inversion in the silicon substrate and also to accumulation in the silicon layer above the insulator, the value of capacitance decreases as the frequency is increased with a voltage fixed. A similar behavior of capacitance in relation to frequency is also observed in the region of positive voltages (>8 V), where the silicon layer becomes depleted while the silicon substrate is in a state of enrichment with majority charge carriers. This is indicative of the presence of surface states at the corresponding Si/SiO$_2$ interfaces. The $G-V$ characteristics shown in Fig. 4b exhibit peaks of capacitive conductance, which also indicates that there are surface

states. The intensity of the conductance peaks corresponding to the bonding interface of SOI structure changes only slightly as the frequency is increased, whereas the intensity of peaks corresponding to the thermal Si/SiO$_2$ interface increases by a factor of 2 as the frequency is increased in the indicated range. As the frequency is increased, a small shift of the position of the conductance peaks along the voltage axis is also observed. This is indicative of the dependence of the density of surface states on energy in the band gap. It is noteworthy that the peaks do not overlap even at the highest frequencies, which is indicative of a weak interaction between surface potentials at two Si/SiO$_2$ interfaces. Similar measurements were also performed for the structures that contained nitrogen in the buried oxide.

In Fig. 5, we show the curves of capacitive conductance measured at the frequency of 1 kHz in relation to the voltage at aluminum electrode for different doses of N$^+$ ions with the energy of 40 keV implanted into the buried SiO$_2$ layer (Fig. 5a) and also for different energies of nitrogen ions implanted with the dose of 3×10^{15} cm^{-2} (Fig. 5b). It can be seen from Fig. 5a that the peak of conductance in the structures that were not nitrogenated is observed at biases of ~10 V; this corresponds to the mode of depletion in the silicon layer. After implantation of low doses of nitrogen ions, the conductance peak is dominant in the region of positive biases; the position of this peak corresponds to the mode of pronounced inversion. As the dose of ions is increased to 3×10^{15} cm^{-2}, the conductance peak becomes bimodal. In addition to the dominant peak of conductance in the region of inversion in the silicon layer on the insulator, a less intense shoulder appears in the region of voltages ~11 V corresponding to the depletion mode for the layer. A further increase in the dose of nitrogen ions is accompanied by attenuation of the high-voltage peak of conductance and by an increase in the intensity of the peak located in the region of 10 V. In addition, position of the latter peak becomes close to the position of the conductance peak for the structure that were not nitrogenated. The corresponding conductance peaks behave similarly in relation to the energy of nitrogen ions (Fig. 5b). In this case, as the energy of N$^+$ ions is lowered from 40 to 20 keV, the intensity of the high-voltage peak of conductance (near 15 V) decreases whereas the intensity of the low-voltage peak (near 10 V) increases. The obtained data indicate that there are two types of traps for charges. In the depletion region, the capacitive conductance is controlled by interaction of majority charge carriers (electrons) with capture centers, whereas the generation−recombination processes are governed by minority charge carriers (i.e., holes) in the region of inversion.

An analysis of the density of states at the interfaces in an SOI structure can be performed on the basis of

Table 2. The values of the flat-band voltage (V_{FB1} and V_{FB2}), the density of fixed charge (Q_{f1} and Q_{f2}), and the cross section σ_{n1} for the capture of majority charge carriers by the states at the interfaces of the SOI structures, which include the buried SiO$_2$ layer; the structures were first implanted with N$^+$ ions with energies of 40, 30, and 20 keV and the dose 3×10^{15} cm^{-2} and were then annealed for 1 h at 1000°C

Energy of N$^+$ ions, keV	V_{FB1}, V	V_{FB2}, V	Q_{f1}, 10^{11} cm^{-2}	Q_{f2}, 10^{11} cm^{-2}	σ_{n1}, cm^2
0	8.1	−5.3	6.1	3.9	7.0×10^{-13}
40	9.1	−4.6	7.0	3.3	9.0×10^{-15}
30	8.3	−4.2	6.4	3.0	3.4×10^{-15}
20	7.3	−4.2	5.7	3.0	9.5×10^{-16}

frequency dependences of a maximum in the capacitive conductance and corresponding capacitance [21]:

$$Q_{it} = \left(\frac{2}{qS}\right)\left(\frac{G_m}{\omega}\right)\Big/\left[\left(\frac{G_m}{\omega C_{ox}}\right)^2 + \left(1 - \frac{C_m}{C_{ox}}\right)^2\right]; \quad (9)$$
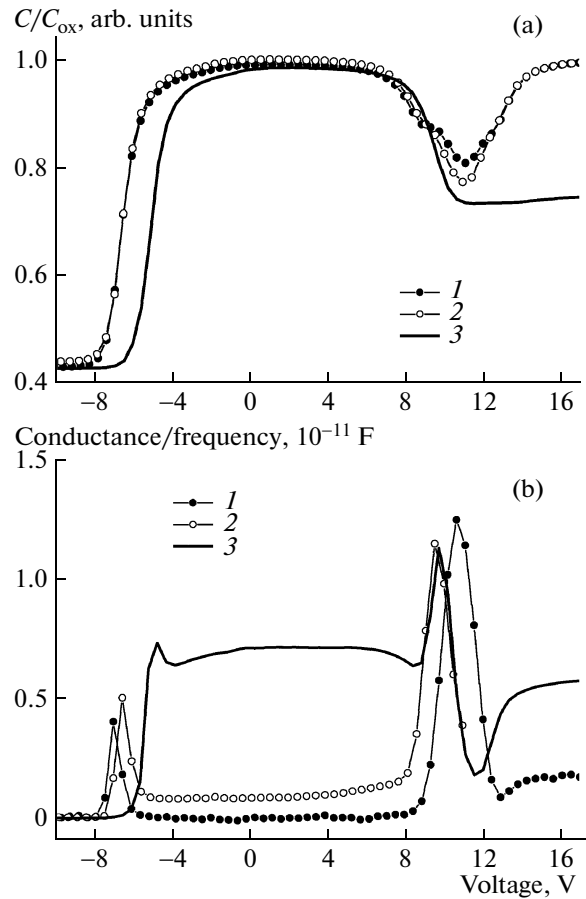

Fig. 4. The (a) $C{-}V$ and (b) $G{-}V$ characteristics of the Al/n-Si/SiO$_2$/n-Si/Al structures that do not contain nitrogen in the buried oxide; the characteristics were measured at the frequencies (*1*) 5×10^2, (*2*) 5×10^3, and (*3*) 5×10^5 Hz.

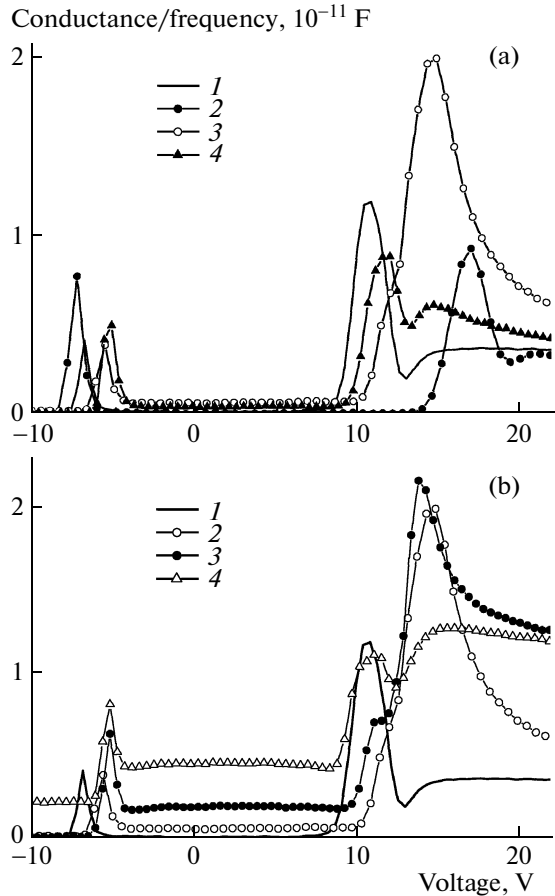Conductance/frequency, 10^{-11} F

Fig. 5. The G–V characteristics of the Al/n-Si/SiO$_2$/n-Si/Al structures with the SiO$_2$ layer (*1*) without introduced nitrogen and the layer implanted with N$^+$ ions (a) with the energy 40 keV and a dose of (*2*) 1×10^{15}, (*3*) 3×10^{15}, and (*4*) 6×10^{15} cm^{-2}; (b) with the dose of N$^+$ ions 3×10^{15} cm^{-2} and the energy of ions (*2*) 20, (*3*) 30, and (*4*) 40 keV. The frequency of measurements was 10^3 Hz.

here, $\omega = 2\pi f$ is the cyclic frequency, f is the frequency of measurement, S is the area of the aluminum electrode, G_m is the value of capacitive conductance measured at the maximum, and C_m is the capacitance corresponding to the value of G_m. Overlap of surface potentials at interfaces of the SOI structure is not taken into account in expression (9). However, in the mode of depletion of the silicon layer of majority charge carriers, which is precisely where the conductance peaks are observed, the substrate is in the state of accumulation, i.e., the effect of thermal interface is completely insignificant in this case. According to the published data [18], an error in determination of the density of surface states with the coefficient of overlap of surface potentials disregarded amounts to ~10%.

In Fig. 6, we show the distribution of the density of surface states in the upper half of the band gap as obtained by the method of conductance at the bonding

boundary of the SOI structure for various values of doses (Fig. 6a) and energies (Fig. 6b) of N$^+$ ions implanted into the buried layer of silicon oxide. The depth of the levels $E - E_i$ (E_i is the midgap of silicon) was calculated for the values of the surface potential at which a maximum of the capacitive conductance was attained. The surface potential ψ_s can be determined from the low-frequency C–V characteristic in the case where the condition for equilibrium is satisfied at a specified frequency. In the case under consideration, we used the data of C–V measurements at a frequency of 100 Hz to determine the surface potential at the bonding boundary. The expression $d\psi_s/dV = 1 - C/C_{ox}$ was integrated in the range of voltages from V_{FB}, where the surface potential is equal to zero, to $V = V_i$ at which inversion sets in:

$$\psi_s = \int_{V_{FB}}^{V_i} (1 - C/C_{ox}) dV. \qquad (10)$$

The effective density of surface states, which corresponds to the peak with the energy $E - E_i$ (Fig. 6), makes it possible to obtain the total density of surface states in the band gap by integrating the curves in Fig. 6 over the entire band gap.

We can use the data of capacitive conductance in relation to frequency to determine the characteristic times of recombination–generation processes τ_R with involvement of surface states at the bonding boundary. The capacitive conductance attains a maximum when $\omega\tau_R = 1$. In the case of n-type conductivity, the quantity τ_R (τ_{Rn}) can be described by the following expression [20]:

$$\tau_{Rn} = \frac{1}{\overline{v}\sigma_n N_D} \exp[q\psi_s/kT]; \qquad (11)$$

here, $\overline{v} = \sqrt{3kT/m_e}$ is the average thermal velocity, m_e is the electron mass, σ_n is the cross section for capture of electrons, T is temperature, and k is the Boltzmann constant. It can be seen from expression (11) that, at the zero surface potential, the cross section for capture of charge carriers is inversely proportional to the constant of the generation–recombination processes. Thus, by plotting the dependence of τ_{Rn} on ψ_s, we estimated cross sections for capture of electrons by surface states at the bonding boundary in relation to the dose and energy of implanted nitrogen ions. The corresponding values are listed in Table 1. It can be seen that, as the concentration of nitrogen atoms within the buried oxide increases, the cross section for capture of majority charge carriers at the bonding boundary decreases by more than two orders of magnitude. If the energy of N$^+$ ions is lowered to 20 keV (and the nitrogen-containing layer approaches the Si/SiO$_2$ interface), the decrease in σ_n (compared to the case of non-nitrogenated bonding boundary) can be as large as three orders of magnitude (Table 2).
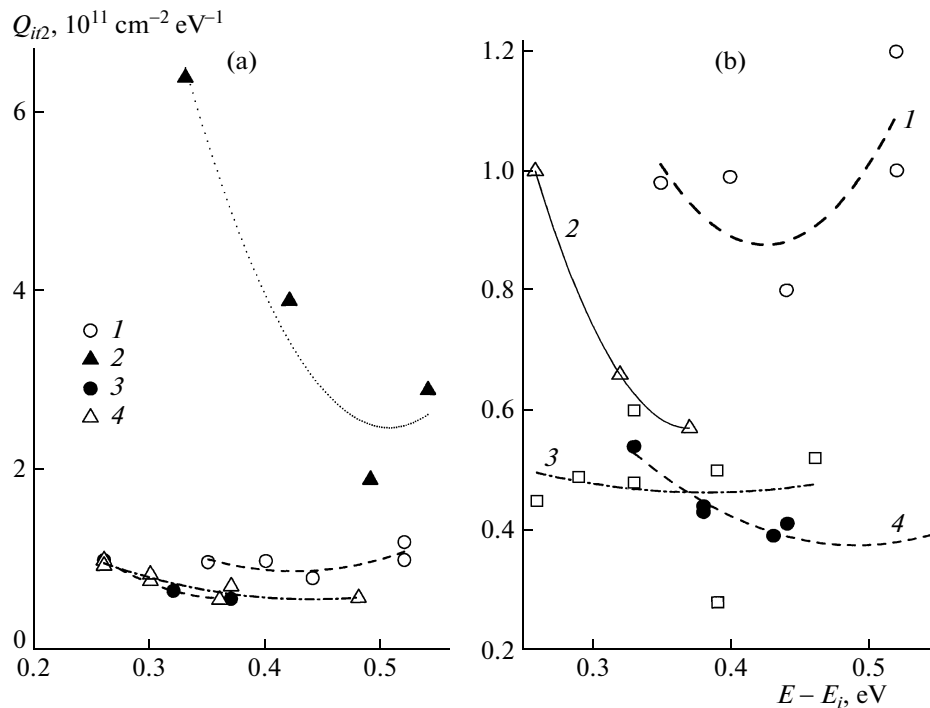
Fig. 6. The distribution of the density of surface states in the upper half of the band gap as obtained by the method of conductance at the bonding boundary of the SOI structure for various values of (a) doses and (b) energies of N^+ ions implanted into the buried layer of silicon oxide. (a) Nitrogen ions with the energy 40 keV and the doses (*1*) 0, (*2*) 1×10^{15}, (*3*) 3×10^{15}, and (*4*) 6×10^{15} cm^{-2}; (b) the dose of N^+ ions is 3×10^{15} cm^{-2} and the ion energies are (*1*) 0, (*2*) 40, (*3*) 30, and (*4*) 20 keV.

The obtained data show that the effective density of surface states at the bonding boundary features the same dependence on the dose and energy of N^+ ions as does the fixed charge in the oxide. An increase in the dose of nitrogen ions or a decrease in their energy is accompanied by an increase in the concentration of nitrogen atoms near the bonding boundary and brings about a decrease in the density of surface states by the factor of 2. This result can be accounted for by saturation of dangling bonds at the Si/SiO$_2$ interface due to incorporation of nitrogen atoms and formation of a subnanometer layer of silicon oxynitride in the region of the bonding boundary.

5. CONCLUSIONS

We used the methods of the $C-V$ and $G-V$ characteristics to study the electrical properties of silicon-on-insulator structures with a buried SiO$_2$ layer implanted with nitrogen ions in relation to the dose and energy of ions. It is established that implantation of low doses of N^+ ions ($<3 \times 10^{15}$ cm^{-2}) stimulates the growth of positive built-in charge in the oxide near the Si/SiO$_2$ interfaces and enhances the density of surface states. An increase in the nitrogen dose ($>3 \times 10^{15}$ cm^{-2}) or a decrease in the ion energy leads to a decrease in the fixed positive charge in the oxide and to a decrease in the density of surface states by a factor of 2. It is

shown that the effective cross section for capture of majority charge carriers by surface states decreases by two to three orders of magnitude as the nitrogen concentration is increased near the Si/SiO$_2$ interface. The obtained results are accounted for by interaction of nitrogen atoms with excess silicon atoms near the Si/SiO$_2$ interface; by elimination of Si–Si bonds, which are traps of positive charges; and by saturation of dangling bonds at the bonding boundary.

REFERENCES

1. M. V. Fischetti, J. Appl. Phys. **57**, 2860 (1985).
2. V. A. Gritsenko, Usp. Fiz. Nauk **178**, 727 (2008) [Phys. Usp. **51**, 699 (2008)].
3. M. Y. Hao, W. M. Chen, K. Lai, and J. C. Lee, Appl. Phys. Lett. **66**, 1126 (1995).
4. S. B. Kang, S. O. Kim, J.-S. Byun, and H. J. Kim, Appl. Phys. Lett. **65**, 2448 (1994).
5. E. C. Carr and R. A. Buhrman, Appl. Phys. Lett. **63**, 54 (1993).
6. Z. Q. Yao, H. B. Harrison, S. Dimitrijev, and D. Sweatman, Appl. Phys. Lett. **64**, 3584 (1994).

7. W. B. Yi, E. X. Zhang, M. Chen, N. Li, G. Q. Zhang, Z. L. Liu, and X. Wang, Semicond. Sci. Technol. **19**, 571 (2004).

8. M. L. Green, D. Brasen, K. W. Evans-Lutterodt, L. C. Feldman, K. Krish, W. Lennard, H.-T. Tang, L. Manhanda, and M.-T. Tang, Appl. Phys. Lett. **65**, 849 (1994).

9. S. K. Dixit, S. Dhar, J. Rozen, S. Wang, R. D. Schrimpf, D. M. Fleetwood, S. T. Pantelides, J. R. Williams, and L. C. Feldman, IEEE Trans. Nucl. Sci. **53**, 3687 (2006).

10. C. W. Perkins, K. G. Aubuchon, and H. G. Dill, IEEE Trans. Nucl. Sci. **15**, 176 (1968).

11. D. Neamen, W. Sheold, and B. Buchanau, IEEE Trans. Nucl. Sci. **22**, 2203 (1975).

12. P. L. F. Hemment, Mater. Res. Soc. Symp. Proc. **33**, 41 (1984).

13. K. J. Reeson, Nucl. Instrum. Methods Phys. Res. B **19–20**, 269 (1987).

14. W. Skorupa and K. Wollschlager, Nucl. Instrum. Methods Phys. Res. B **32**, 440 (1988).

15. K. J. Reeson, P. L. F. Hemment, C. D. Meekison, C. D. Marsh, G. R. Booker, R. J. Chater, J. A. Kilner, and J. Davis, Nucl. Instrum. Methods Phys. Res. B **32**, 427 (1988).

16. A. B. Danilin, K. A. Drakin, V. V. Kukin, A. A. Malinin, V. N. Mordkovich, A. F. Petrov, V. V. Saraykin, and O. I. Vyletalina, Nucl. Instrum. Methods Phys. Res. B **58**, 191 (1991).

17. E. Zhang, W. Yi, J. Chen, Zh. Zhang, and X. Wang, Smart Mater. Struct. **14**, N 42 (2005).

18. H.-S. Chen and S. S. Li, IEEE Trans. Electron. Dev. **39**, 1740 (1992).

19. S. Cristoloveanu and S. S. Li, *Electrical Characterization of Silicon-on-Insulator Materials and Devices* (Kluver Acad., Boston, Dordrecht, London, 1995).

20. E. N. Nicollian and J. R. Brews, *MOS (Metal–Oxide–Semiconductor) Physics and Technology* (Wiley, New York, 1982).

21. W. A. Hill and C. C. Coleman, Solid State Electron. **23**, 987 (1980).

Translated by A. Spitsyn